

On the Radii of Extrasolar Giant Planets

Peter Bodenheimer

Gregory Laughlin

Douglas N. C. Lin

UCO/Lick Observatory, University of California, Santa Cruz, CA 95064

ABSTRACT

We have computed evolutionary models for extrasolar planets which range in mass from $0.1 M_{\text{JUP}}$ to $3.0 M_{\text{JUP}}$, and which range in equilibrium temperature from 113 K to 2000 K. We present four sequences of models, designed to show the structural effects of a solid ($20 M_{\oplus}$) core and of internal heating due to the conversion of kinetic to thermal energy at pressures of tens of bars. The model radii at ages of 4–5 Gyr are intended for future comparisons with radii derived from observations of transiting extrasolar planets. To provide such comparisons, we expect that of order 10 transiting planets with orbital periods less than 200 days can be detected around bright ($V < 10 - 11$) main-sequence stars for which accurate well-sampled radial velocity (RV) measurements can also be readily accumulated. Through these observations, structural properties of the planets will be derivable, particularly for low-mass, high-temperature planets. Implications regarding the transiting companion to OGLE-TR-56 recently announced by Konacki et al. are discussed.

With regard to the transiting planet, HD 209458b, we find, in accordance with other recent calculations, that models without internal heating predict a radius that is $\sim 0.3 R_{\text{JUP}}$ smaller than the observed radius. Two resolutions have been proposed for this discrepancy. Guillot & Showman hypothesize that deposition of kinetic wind energy at pressures of tens of bars is responsible for heating the planet and maintaining its large size. Our models confirm that dissipation of the type proposed by Guillot & Showman can indeed produce a large radius for HD 209458b. Bodenheimer, Lin & Mardling suggest that HD 209458b owes its large size to dissipation of energy arising from ongoing tidal circularization of the planetary orbit. This mechanism requires the presence of an additional planetary companion to continuously force the eccentricity. We show that residual scatter in the current RV data set for HD 209458b is consistent with the presence of an as-of-yet undetected second companion, and that further RV monitoring of HD 209458 is indicated.

Tidal circularization theory also can provide constraints on planetary radii. Extrasolar giant planets with periods of order 7 days should be actively circularizing. We find that the observed eccentricities of $e \sim 0.14$ for both HD 217107b ($P = 6.276$ d; $M \sin i = 1.80 M_{\text{JUP}}$), and for HD 68988b ($P = 7.125$ d, $M \sin i = 1.29 M_{\text{JUP}}$) likely

indicate either relatively small planetary radii for these objects ($R \sim 1.1 R_{\text{JUP}}$) or tidal quality factors in the neighborhood of $Q_{\text{P}} \sim 10^7$. For these two planets, it will be difficult to differentiate the contribution from tidal and kinetic heating. But the radius of HD 168746b ($P = 6.403$ d, $M \sin i = 0.23 M_{\text{JUP}}$) is sensitive to whether the planet’s interior is heated by tidal dissipation or kinetic heating. The tidal circularization time scale of this planet is shorter than the age of its host star, but we show that within the observational uncertainties, the published RV data can also be fit with a circular orbit for this planet. As more RV planets with periods of order a week are discovered, $Q_{\text{P}}(T_{\text{eq}}, M_{\text{P}})$ and $R_{\text{P}}(T_{\text{eq}}, M_{\text{P}})$ will become better determined.

Subject headings: planetary systems – planets and satellites: general

1. Introduction

Astronomers are understandably enthusiastic about the prospect of detecting Jovian-type planets transiting bright ($V < 10$) chromospherically quiet late-type stars. A bright parent star allows highly accurate orbital parameters to be deduced from Doppler RV measurements, while the transit phenomenon affords direct measurements of the planetary parameters.

Indeed, the celebrated occultations of HD 209458 ($V=7.65$) (Charbonneau et al. 2000, Henry et al. 2000) have provided a scientific bonanza. The identification of this transit allowed detailed follow-up measurements, including direct and accurate measurements of the planet’s radius ($1.35 \pm 0.06 R_{\text{JUP}}$ [Brown et al. 2001]; $1.41 \pm 0.10 R_{\text{JUP}}$ [Cody & Sasselov 2002]), mass ($0.69 \pm 0.05 M_{\text{JUP}}$; [Mazeh et al. 2000]), and even the presence of sodium in its atmosphere (Charbonneau et al. 2002).

Following the discovery of 51 Peg (Mayor & Queloz 1995), theoretical models of Jovian-mass planets subject to strong irradiation were computed (Guillot et al. 1996). These models predicted that short-period Jovian planets with equilibrium temperatures of 1300–1400 K at ages of several Gyr would be significantly larger than Jupiter. The discovery that HD 209458b has a large radius initially seemed to be a strong confirmation of these models (Burrows et al. 2000).

While the large observed size of HD 209458b certainly suggests that it is a gas-giant composed primarily of hydrogen, recent work by Guillot & Showman (2002) indicates that a serious gap exists in our understanding of irradiated giant planets. They show that standard evolutionary models can recover the observed radius of HD 209458b only if the deep atmosphere is unrealistically hot. A more nearly correct treatment of radiative heating leads to more rapid and efficient planetary contraction, and predicted radii which are $0.2\text{--}0.3 R_{\text{JUP}}$ too small, that is, in the range $1.1 R_{\text{JUP}}$ at an age of 5 Gyr. The results of Bodenheimer et al. (2001), based on similar assumptions, also produce radii which are too small.

Two resolutions to this problem have been suggested. Bodenheimer et al. (2001) argue that HD 209458b might be receiving interior tidal heating through ongoing orbital circularization, whereas

Guillot & Showman (2002) propose that strong insolation-driven weather patterns on the planet are leading to some conversion of kinetic wind energy into thermal energy at pressures of tens of bars. At the time the work of Bodenheimer et al. (2001) was done, the eccentricity of HD 209458 was thought to be consistent with zero, thus no obvious source of tidal heating was present. However, as we discuss below, the continued accumulation of RV measurements of HD 209458b will allow for much tighter constraints on the planetary eccentricity and the possible presence of a second planetary companion.

Although there are a number of studies of the evolution of giant planets (for reviews see Hubbard et al. 2002; Burrows et al. 2001), at present there are no published grids of models for planets with equilibrium temperatures in the 500–1000 K regime that are intermediate between Jupiter ($T_{\text{eq}} = 113$ K) and HD 209458b ($T_{\text{eq}} \approx 1350$ K). As we discuss below, we expect that transiting planets with intermediate periods ($10 \text{ d} < P < 200 \text{ d}$) will soon be found. One of the major intents of this paper is to provide predictions for the radii of such planets. Indeed, an accurate size and mass determination for even a single intermediate-period planet will help resolve the size discrepancy observed for HD 209458b. A planet with intermediate period will not be experiencing significant internal tidal dissipation, but would still be irradiated to an extent sufficient to produce a significant amount of kinetic heating from the mechanism suggested by Guillot & Showman (2002). We therefore also wish to show that within certain limits such observations can (1) distinguish between planets with and without a solid core, and (2) show whether or not the kinetic heating mechanism is operating. One possible consequence of such a comparison could be that the kinetic heating mechanism is not effective and that therefore HD 209458b’s radius can only be explained by tidal dissipation. On the other hand, if newly-discovered radii were found to be consistent with kinetic heating, constraints could be placed on the (still not-well understood) tidal heating mechanism.

Intermediate-period planets are also interesting because they can harbor dynamically stable large satellites. Indeed, all satellites larger than $R = 70$ km orbiting a $P = 3$ d Jovian planet are removed over 5 Gyr. However, Mars-mass moons can last for 5 Gyr in the Hill Sphere of a 1 M_{JUP} planet orbiting a 1 M_{\odot} star in a 27 day (0.18 AU) orbit, whereas in a 54 day (0.28 AU) orbit, Earth-mass moons are dynamically stable (Barnes & O’Brien 2002, Evonuk et al. 2003). Brown et al. (2001) report that with HST, detections of satellites as small as 1 R_{\oplus} are feasible. Therefore, the discovery of the transit of an intermediate-period planet could be followed up to search for large moons, and, additionally, planetary rings.

2. Prospects for Detection of Transiting Planets

The *a priori* probability that a planet transits its parent star as seen from the line of sight to Earth is given by,

$$\mathcal{P}_{\text{transit}} = 0.0045 \left(\frac{1\text{AU}}{a} \right) \left(\frac{R_{\star} + R_{\text{pl}}}{R_{\odot}} \right) \left(\frac{1 - e \cos(\pi/2 - \varpi)}{1 - e^2} \right) \quad (1)$$

where a is the semi-major axis of the orbit, R_* and R_{pl} are the radii of the star and planet, respectively, e is the orbital eccentricity, and ϖ is the argument of periastron referenced to the plane of the sky. In order to obtain an accurate mass for a transiting planet, one requires a good set of RV measurements so that an orbit can be fit. Accurate RV measurements are best obtained for bright parent stars, so it is therefore useful to estimate the number of transiting planets that are likely to be available for accurate mass and radius determinations. If one examines the parameters of the current RV planet catalog¹, one finds that among the 16 known planets with periods $P < 10$ d, there are $< n_T > = 1.62$ expected transits, and indeed, within this group, a transiting case (HD 209458b) is known. Twelve of the planets with $P < 10$ d have firm non-detections (including HD 68988b and HD 217107b, whose properties are discussed in more detail below). Of the remaining three planets with $P < 10$ d, one, HD 76700b ($P = 3.971$ d) is currently under surveillance, and two others, HD 162020b ($P = 8.428$ d), and HD 168746 ($P = 6.403$ d) will be evaluated during Spring 2003.

Within the aggregate of 23 known planets having periods in the range $10 \text{ d} < P < 200 \text{ d}$, the expected number of transiting planets is $< n_T > = 0.64$. Very few of the parent stars in this group, however, have been exhaustively monitored for transits. These stars therefore represent excellent targets for a distributed network of small telescopes. We also note that among the 60 known planets with $P > 200$ d, one expects $< n_T > \approx 0.5$ additional transiting planets. Because of the less well-determined orbits for most of these long-period planets, and because of the infrequent occultations, these stars will remain difficult targets to follow up.

In addition to the current census, more planets with periods suitable for the discovery of transits will soon be emerging from the RV surveys. To see this, consider Figure 1, which plots the periods of 98 known extrasolar planets versus the Julian dates on which their discoveries were announced. The magnitudes of the parent stars are color-coded to range from red ($V < 4$) to black ($V > 9$), while the radii of the circles marking each planet are proportional to $(M_P \sin i)^{1/3}$. This diagram shows that the pace of discovery of extrasolar planets with $P < 200$ d is proceeding at a steady rate, while the rate of discovery of planets with $P < 10$ d has begun to peak. Currently, within the $10 \text{ d} < P < 200 \text{ d}$ range, there are five known planets orbiting stars with $V < 6$, seven orbiting stars with $6 < V < 7$, six orbiting stars with $7 < V < 8$, and two planets each in the $8 < V < 9$, and $9 < V < 10$ ranges. If we assume that every available chromospherically quiet main sequence dwarf with $V < 6$ has been adequately surveyed for $P < 200$ d planets, and that each magnitude bin of unit width contains 1.8 times as many stars as available for bin $(V - 1)$, then we expect that roughly $9 + 16 + 29 + 52 = 106$ detectable planets with $10 \text{ d} < P < 200 \text{ d}$ exist in orbit around stars with $V < 10$, indicating that more than 100 additional planets in this category can be detected using current RV techniques for bright stars. Statistically, this implies that 3 intermediate-period RV-detectable transiting planets orbit bright nearby stars. Application of the same argument to planets with $P < 10$ d indicates that 4 short-period transiting planets are

¹see, e.g., <http://www.transitsearch.org/stardatabase/index.htm>

to be expected in orbit around bright stars.

In summary, we can expect to obtain highly accurate radii and masses for only a limited number of planets. This collection will serve as the major observational basis for our understanding of the structure of giant planets. The ten or so transiting planets that we can expect to find will likely span two orders of magnitude in mass ($0.1M_{\text{JUP}} < M_P < 10.0M_{\text{JUP}}$), and a wide range in temperature ($300 \text{ K} < T_{\text{eq}} < 2000 \text{ K}$). In order to interpret this data, it is useful to compute a grid of models spanning mass and equilibrium temperature at the age of a typical planet-bearing star (5 Gyr).

3. Models for Irradiated Giant Planets

Models for the evolution of giant planets of various masses have been computed with a descendant of the Berkeley stellar evolution code (Heney, Forbes, & Gould 1964). This computer program has received a number of modifications and improvements to the input physics during its forty years of existence. It calculates the evolution and mass accretion rate of the gaseous envelope, under the assumption that the planet is spherical, and that the standard equations of stellar structure apply. It has been used to calculate the formation phase of planets in the solar system (Pollack et al. 1996) and of extrasolar planets by Bodenheimer, Hubickyj, & Lissauer (2000). The physical assumptions employed in the calculations are described in those papers. Energy transport occurs either by radiation or convection, according to the Schwarzschild criterion for convection. Energy sources include (1) gravitational contraction, (2) cooling of the interior, and (3) in some cases energy deposition in the atmosphere, at pressures in the range 1 bar to 100 bars, caused by stellar heating (Guillot & Showman 2002). In the outer envelope of the planet, where radiation is likely to be the energy transport mechanism, dust grains are assumed to have settled into the interior and evaporated, so that they contribute negligibly to the opacity. The assumed absence of grains in the envelopes of low-mass objects is consistent with studies of the detailed observed spectra of T-dwarfs (Tsuji 2002). Pure molecular opacities in the temperature range 70-4000 K were obtained from R. Freedman (private communication) for a near-solar composition. Above 4000 K the table from Alexander & Ferguson (1994) was used; however for such temperatures the models are always convective, so the details of the opacity are unimportant. In convection zones, which always include most of the mass of the planet, the temperature gradient is assumed to take the adiabatic value. The equation of state of Saumon, Chabrier, & van Horn (1995) was employed, slightly softened as suggested by Burrows et al. (2000). At the surface, the luminosity is composed of two components: the internal luminosity generated by the planet (L_{int}), and the energy absorbed from the stellar radiation flux and re-radiated (‘insolation’). The boundary conditions at the Rosseland mean photosphere are

$$L_{\text{tot}} = L_{\text{int}} + 4\pi R_P^2 \sigma T_{\text{eq}}^4 \quad (2)$$

$$\bar{\kappa}_{\text{ph}} P_{\text{ph}} = \frac{2}{3} g \quad (3)$$

where L_{tot} is the total luminosity, T_{eq} is the equilibrium temperature defined below in equation (8), $\bar{\kappa}_{\text{ph}}$ is the mean opacity at the photosphere, P_{ph} is the pressure at the photosphere, and g is the surface gravity. Since the details of the atmosphere, including frequency-dependent effects (Chabier & Baraffe 2000), are not taken into account, the radii derived by this procedure should be regarded as preliminary.

In the case of extrasolar planets, it is not known whether or not a central solid/liquid rock/ice core is present; however its presence or absence could be an important clue to the formation mechanism. The composition, density, and mass of the core would depend on the formation and migration history of the planet. In the case of the solar system giant planets it is likely that cores exist; however, the available constraints from observations and modeling still allow a considerable range in their properties (Wuchterl, Guillot, & Lissauer 2000). In the case of Jupiter, the range of possible core masses is 0 to 10 M_{\oplus} , and for Saturn it is 5–15 M_{\oplus} . However these planets also have heavy element abundances in excess of solar abundance ratios in their gaseous envelopes. The total heavy element abundance in Jupiter is thought to be about 30 M_{\oplus} , or 10% of the total mass, while in Saturn it is thought to be about 25% of the total mass. The division of the heavy elements between envelope and core is uncertain mainly because of uncertainties in the Saumon-Chabrier-van Horn equation of state. With these considerations in mind, we made calculations for each mass and temperature both with a core and without a core. The core mass, which is designed to represent approximately the total excess in heavy elements over solar abundance, is taken to be 40 M_{\oplus} in the case of the more massive planets (0.69 M_{JUP} and above) and 20 M_{\oplus} for lower masses. Two cases with a 20 M_{\oplus} core for 0.69 M_{JUP} were also calculated. Models without cores are assumed to have solar composition ($X = .70$, $Y = .28$, $Z = .02$). In the models with cores, the core density is assumed to have a constant value of 5.5 g cm^{-3} , except for the highest mass (3 M_{JUP}), where the high pressures in the center require a higher core density, which we take to be 10.5 g cm^{-3} . The composition of the envelopes of the models with cores is assumed to be solar. For the case of 1 M_{JUP} , calculations were also made with a core density of 10.5 g cm^{-3} ; in an example of a current Jupiter model, Marley (1999) indicates that the range of densities in the core is about 9 to 23 g cm^{-3} . However, much of the heavy-element material in Jupiter is in the envelope at much lower pressures. For the lower masses, a core density of 5.5 g cm^{-3} is thought to be reasonable; Marley’s (1999) Saturn model has a density of 6–7 g cm^{-3} in much of the core. A giant planet with enhanced heavy-element abundance can have a significantly smaller radius than one of the same mass with solar abundance.

The initial condition is a planet of $R \approx 2 R_{\text{JUP}}$ at an age of a few Myr. The planet is assumed to have migrated to its final orbit during the formation phase, thus the assumed equilibrium temperature is constant in time. A calibration run with 1 M_{JUP} with a core and with insolation appropriate to Jupiter at 5 AU ($T_{\text{eq}} = 113$ K) contracted to a final radius of 1 R_{JUP} after an evolution time of 4.5 Gyr. At the final time, the temperature at 1 bar pressure in the atmosphere was about 160 K, in good agreement with observations of Jupiter.

For each value assumed for the planet mass (0.11, 0.23, 0.69, 1.00, and 3.0 M_{JUP}), the models

in Table 1 illustrate how the presence of a solid core, as well as the assumed value of T_{eq} , affects the planetary radius (given in R_{JUP}). In this table, as well as in Table 2, the core densities are 5.5 g cm^{-3} for all cases except $3.0 M_{\text{JUP}}$, where it is 10.5 g cm^{-3} . Table 2 presents an exactly analogous sequence of models which also include an energy source term (in addition to the direct radiative heating of the atmosphere), applied as described by Guillot & Showman (2002). This source term deposits 1.7% of the incoming stellar flux in the regions of the planetary envelope where the pressure is tens of bars. The energy deposition fraction of 1.7% was obtained through calibration runs in which the fraction was varied until the radius of HD 209458 was reproduced. Specifically, with that fraction, for the case of $0.69 M_{\text{JUP}}$, without a core and with $T_{\text{eq}} = 1300 \text{ K}$, a radius of $1.37 R_{\text{JUP}}$ was obtained at an age of 4.5 Gyr. For all other models, the same fraction of the incident stellar radiation was assumed to be converted to heat at pressure levels from the surface down to $\sim 100 \text{ bar}$, with an exponential fall-off of heating with depth. The incident stellar radiation is of course proportional to the projected area of the planet’s star-facing hemisphere; this effect was taken into account during the contraction.

The radii of these models show in many cases observably large variations as the underlying physical parameters (i.e. presence of a core or energy deposition via kinetic heating) are varied. It is therefore likely that the discovery of several more transiting extrasolar planets will make it clear whether giant planets have solid cores, and whether they generally have access to an interior energy source such as the kinetic heating described by Guillot & Showman (2002). We note that the delineation between individual modes is especially clear for both the hotter and the lower-mass planets. For a low-mass relatively short-period planet such as HD 168746b with $M \sin i = 0.23 M_{\text{JUP}}$, $T_{\text{eq}} = 1000 \text{ K}$, and $P = 6.4 \text{ days}$, the two models without kinetic heating have final radii of 0.90 and $1.07 R_{\text{JUP}}$ for cases with a core and without a core, respectively, and the two corresponding models with kinetic heating have radii of 1.34 and $1.53 R_{\text{JUP}}$, respectively. The four possibilities should be cleanly separable observationally, as the observational uncertainty is about $0.1 R_{\text{JUP}}$. In the case of a planet with $0.11 M_{\text{JUP}}$ (cf. HD 49674), the effect becomes even larger, with observationally separable differences among the four cases out to $T_{\text{eq}} = 500 \text{ K}$ (about 0.4 AU for a solar-type star). In the case with a core, this model is intermediate between a Saturn-type and a Neptune-type planet, with an envelope mass of $15 M_{\oplus}$ and a core mass of $20 M_{\oplus}$.

It is important to note, however, that for a planet as massive as $3 M_{\text{JUP}}$ it is not possible to observationally distinguish between these various cases, except that at very short periods with $T_{\text{eq}} = 1500$ or 2000 K , it may be possible to determine whether or not kinetic heating is occurring. For $1 M_{\text{JUP}}$ it is in general not possible to distinguish between planets with or without cores; for the calculations without kinetic heating the difference is only about 5%. It is, however, possible to distinguish between planets with or without kinetic heating if the equilibrium temperature is above about 1200 K . Models with $1 M_{\text{JUP}}$ have also been calculated with a core density of 10.5 g cm^{-3} . Their radii are close to 3% smaller in all cases (with or without kinetic heating) than in the case with a density of 5.5 g cm^{-3} , making the difference in radius between a planet with and without a core marginally detectable in some cases. In the case of $0.69 M_{\text{JUP}}$, planets with or without cores

are only marginally separable, while planets with or without kinetic heating are cleanly separable down to $T_{\text{eq}} = 1000$ K. Calculations were also made for $0.69 M_{\text{JUP}}$ with a core of $20 M_{\oplus}$, with and without kinetic heating and with $T_{\text{eq}} = 1000$ K. The radii turned out to be 1.06 and 1.22 R_{JUP} , respectively, intermediate between the values for the case without a core and for the case with a core of $40 M_{\oplus}$. In this situation the presence of a core could not be detected, but the effect of kinetic heating could still be clearly discerned.

4. Constraints Provided by the Current Planetary Census

While additional transiting planets will certainly be of immense importance in clarifying the structural theory of extrasolar giant planets, there is interesting information which can be gleaned from the current census of extrasolar planets. We now use the planet models which were described in the previous section to examine a number of interesting individual cases.

4.1. HD 209458b

As Table 1 shows, a standard model for $M = 0.69 M_{\text{JUP}}$ without a core at $T_{\text{eq}} = 1300\text{K}$ has a radius of only 1.12 R_{JUP} ; the model with a core is even smaller. Bodenheimer, Lin & Mardling (2001) suggest that internal dissipation of tidal energy arising from orbital circularization is responsible for the large observed size of HD 209458b. If HD 209458b is unperturbed by a third body, then tidal dissipation will circularize its orbit on a timescale (Goldreich & Soter 1966)

$$\tau_{\text{circ}} = \frac{e}{\dot{e}} = \left(\frac{4Q_{\text{P}}}{63n} \right) \left(\frac{M_{\text{P}}}{M_{\star}} \right) \left(\frac{a}{R_{\text{P}}} \right)^5 = 0.082 \left(\frac{Q_{\text{P}}}{10^6} \right) \text{Gyr}, \quad (4)$$

where $n = 2\pi/P = 1.783$ rad/d is the planet’s mean motion, $M_{\star} = 1.1M_{\odot}$ is the stellar mass, and Q_{P} is the tidal quality factor. Q_{P} is associated with substantial uncertainty. Based on the Jupiter-Io interaction, Q_{JUP} is estimated to lie in the range $6 \times 10^4 - 2 \times 10^6$ (Yoder & Peale 1981). Onset of tidal circularization among main-sequence binaries suggests that the Q -value for stars is of order 10^6 (Terquem et al. 1998). The Q_{P} values for extrasolar planets are likely to be strong functions of planetary mass, temperature, and composition. As more planets are found with periods, $P \sim 7\text{d}$, the range of Q_{P} values appropriate to moderately irradiated planets of a range of masses will become better determined.

The rate of internal energy dissipation is given by,

$$\dot{E}_d = \frac{e^2 G M_{\star} M_{\text{P}}}{a \tau_{\text{circ}}}, \quad (5)$$

which for HD 209458b is

$$\dot{E}_d = 1 \times 10^{29} e^2 \left(\frac{10^6}{Q_{\text{P}}} \right) \text{ erg s}^{-1}. \quad (6)$$

To estimate this rate for particular choices of Q_P , we need to estimate the orbital eccentricity for HD 209458b.

To date, the UC-Keck Planet Search has obtained RV measurements of HD 209458 which fall in 33 distinct 2-hour time bins. These updated velocities have been provided by G. Marcy (2002, personal communication). Among these 33 binned observations, 3 have photon-weighted epochs which fall within the periodic transit window for HD 209458b. Radial velocity measurements taken during transit are seriously affected by asymmetric distortions in the stellar line profiles arising from the planet occulting a rotating star (Bundy & Marcy 2000, Queloz et al. 2000). We therefore remove these three points from the RV data set and use a Levenberg-Marquardt algorithm (Press et al. 1992) to fit a Keplerian orbit to the remaining velocities. Repeated observations of the HD 209458b transits which include mid-1990’s data from the Hipparcos epoch photometry (Castellano et al. 2000, Robinchon & Arenou 2000), HST/STIS observations by Brown et al. (2001), and HST/FGS observations by Welsh et al. (2003) have allowed the planetary period and the transit midpoint to be determined to high accuracy. Welsh et al. (2003) report a period $P = 3.5247542 \pm 4.4 \times 10^{-6}$ HJD and a transit midpoint $T_c = 2452223.89617 \pm 8.6 \times 10^{-5}$ HJD. With this ephemeris, and for any given choice of the planetary e and ϖ , we can compute the mean anomaly M at the epoch of the first data point (JD=2451341.120). We fit for (1) the planetary eccentricity e , (2) the argument of perihelion ϖ , (3) the planetary $M \sin i$, and (4) the velocity zero-point for the data set. This four-parameter variation returns a best-fit system having $e = 0.033$, $\varpi = 67.17$, $M \sin i = 0.679 M_{JUP}$, and $\Delta v = 5.36$ m/s. The fit has a $\sqrt{\chi^2} = 1.69$, and an rms scatter of 8.05 m/s. If the eccentricity for the planet is forced to be zero and the velocities are re-fit for M , $M \sin i$, and Δv_1 , we obtain a best fit having $M \sin i = 0.652$, and $\Delta v_1 = 4.74$ with an rms scatter of 8.31 m/s. These results are in excellent agreement with those obtained by Marcy (2002; personal communication) who finds a best-fit eccentricity $e = 0.028 \pm 0.012$ using an independent code.

The measured eccentricity of $e \sim 0.03$ in the one-planet fit to the HD 209458b RV data therefore appears to have some statistical significance. For $e = 0.03$, the rate of energy dissipation in HD 209458b is $\dot{E} = 1.0 \times 10^{26} (\frac{10^6}{Q_P})$ erg s $^{-1}$. A new model calculation was made for the evolution of 0.69 M_{JUP} at $T_{eq} = 1300$ K including tidal dissipation energy distributed uniformly in mass throughout the gaseous region of the planet. It was determined that a no-core model requires internal tidal heating of $\dot{E}_d \approx 4 \times 10^{26}$ erg s $^{-1}$ to achieve a radius $R = 1.35 R_{JUP}$. Therefore, if the best-fit eccentricity is secure, and if HD 209458b contains no core, the observed radius can be explained by tidal dissipation if $Q_P \approx 2.5 \times 10^5$, well within the range derived for Jupiter. The required dissipation is higher than that quoted by Bodenheimer et al. (2001) because of changes in the equation of state and opacity since that time. Also, for a model with a core, internal heating of $\approx 4 \times 10^{27}$ erg s $^{-1}$ is required to maintain the same radius. This amount of heating would require, for the same value of Q_P , an eccentricity $e \approx 0.1$, a value which appears to be incompatible with the RV data set.

Any non-zero eccentricity for HD 209458b implies that some mechanism exists to excite eccentricity, since the circularization e-folding time $\frac{e}{\dot{e}} \sim 10^8$ years is considerably shorter than the

estimated system age of 4.5 Gyr (Mazeh et al. 2000). Bodenheimer et al. (2001) suggest that the eccentricity of HD 209458b could be forced by an additional planetary companion, and this process does seem to be occurring in the multiple system ν And. Here we examine whether the residual scatter in the HD 209458 RV data set can admit a second planet which is capable of forcing a time-averaged eccentricity $\bar{e} \sim 0.03$ for HD 209458b.

Figure 2 shows a Lomb-Scargle (Press et al. 1992) periodogram of the RV residuals after the RV contribution due to our 1-planet ($e=0.033$) fit has been subtracted. The Lomb-Scargle periodogram is optimized to detect periodicities in unevenly sampled data, and is described in detail by Scargle (1982). In our periodogram, modest peaks remain at 365 and 80 day periodicities. The 365 day periodicity is certainly an aliasing peak arising from the 1-year observing cycle. If we make the hypothesis that the 80 day peak arises from a second companion, we estimate the $M \sin i$ of this second planet to be $\sim 0.12 M_{\text{JUP}}$, in order to model the 6.0 m/s scatter which is unaccounted for by the rms instrumental error of 4.8 m/s and an assumed stellar jitter of $\langle j \rangle = 4.0$ m/s. This estimate for stellar jitter is based on values reported for several similarly old, chromospherically quiet G stars (Saar, Butler, & Marcy 1998), and could be significantly larger.

We have performed four self-consistent 2-planet fits to the velocities (see Laughlin & Chambers 2001). In the first three fits, we constrain the parameters of the hypothetical second planet “c” by fixing the argument of periastron $\varpi_c = 60.5^\circ$, and $M_c \sin(i) = 0.127 M_{\text{JUP}}$, and assuming eccentricity values (i) $e_c = 0.0$, (ii) $e_c = 0.2$, and (iii) $e_c = 0.4$. The parameters of the inner planet “b” are allowed to vary as explained above. The mean anomaly at the epoch of the first data point and the period of the hypothetical planet “c” are allowed to vary. These fits are listed as fits(1-3) in Table 3. In each case, the fitted period is $P_c \sim 84$ d. We find that all three fits can self consistently reduce the excess scatter to that expected from instrumental noise, added in quadrature to a stellar jitter of $\langle j \rangle = 4.1$ m/s for $e_c = 0.4$, $\langle j \rangle = 4.2$ m/s for $e_c = 0.2$, and $\langle j \rangle = 4.3$ m/s for $e_c = 0.0$. We also performed a fit to the RV data in which we allowed all of the parameters of the hypothetical planet “c” to vary, including the mass and the eccentricity. The resulting system produced an extremely close fit to the data, requiring $\langle j \rangle = 1.7$ m/s, which is almost certainly smaller than the velocity jitter of the star. In this fourth model, listed as fit 4 in Table 3, the eccentricity of “c” is 0.7, and the mass has increased to $0.22 M_{\text{JUP}}$. It is important to stress that these fits illustrate only the existence of models that provide a consistent explanation of the stellar RV variations. They by no means constitute the detection of a second planetary companion.

We next examine the dynamical consequences arising from the presence of a second planet in the HD 209458 system. For concreteness, we use our fit in which the eccentricity of the hypothetical second planet is fixed at $e_c = 0.4$. Inclusion of this second planet causes the fitted eccentricity of HD 209458b to decline to $e_b = 0.019$. Fischer et al. (2001) have noted that the inclusion of a second planet into a RV fit generally causes the fitted eccentricity of the first planet to decline.

In order to examine the degree of eccentricity exchange between planet “b” and the hypothetical planet “c”, we start with the osculating orbital elements reported in Table 3 for the trial

self-consistent 2-planet fit having $e_c = 0.4$, and integrate the system forward in time using the Burlirsch-Stoer method.

We note that in the absence of relativistic advance of the perihelion of planet HD 209458b, the Laplace-Lagrange secular exchange of angular momentum (e.g. Murray & Dermott 1999) is quite strong – the eccentricity of planet “b” oscillates between 0.018 and 0.14 with a period of $P \sim 40,000$ years. Relativistic apse precession, however, detunes the secular exchange and reduces the time-averaged \bar{e} to 0.03 (see also Mardling & Lin 2002). The results are shown in Figure 3. The two planets experience an apsidal lock when relativistic apse precession is included, but this lock is not required for the secular eccentricity exchange to occur. Note that while the ratio of the total angular momenta $L_b/L_c \sim 1.6$ is not far from unity, the larger eccentricity excursions for planet “b” occur because its eccentricity is smaller. That is, given that the orbital angular momentum of a planet is

$$L_P = \frac{M_P M_\star}{M_P + M_\star} a^2 n (1 - e^2)^{1/2}, \quad (7)$$

and that the total angular momentum $L = L_b + L_c$ is conserved, the $(1 - e^2)^{1/2}$ dependence in the above equation demands larger eccentricity variations for the planet with smaller eccentricity.

As discussed above, our evolutionary models show that \dot{E} for $\bar{e} = 0.03$ produces sufficient heating in the planet to account for the observed radius in the event that the planet contains no core and $Q_P \approx 2.5 \times 10^5$.

The rms RV measurement errors for HD 209458b are $\langle \sigma \rangle = 4.86$ m/s, and so as more RVs are obtained for this star, the presence of a second companion of the type described here should be confirmed or ruled out. The potential detectability of the perturbing companion “c” is aided by the requirement that its period should be less than the current ~ 1200 day duration of the RV data set. HD 209458 shows a RV trend of only 0.0007 ± 0.002 $\text{ms}^{-1}\text{d}^{-1}$. Trial calculations of secular eccentricity exchange indicate that an exterior planet producing a linear 0.0007 $\text{ms}^{-1}\text{d}^{-1}$ velocity trend is not large enough to maintain a significant time-averaged eccentricity for planet HD 209458b. Hence the perturbing companion, if it exists, has a period short enough to average out a residual trend over a 4-year time frame. The hypothetical $P = 80$ d planets considered above easily fulfill this condition.

The current Keck Planet Search RV data set for HD 209458b contains only 33 binned RVs, which means that a significant improvement of the system characterization can be obtained over the next several years if frequent additional measurements are made. Because individual high-precision RV measurements are expensive, it is therefore useful to examine how the detectability of a hypothetical HD 209458 “c” improves as more RV measurements are taken.

To do this, we have taken the hypothetical 2-planet system shown in fit 3 of Table 3, and integrated it forward through JD 2453266 (September 2004). We then generated a simulated campaign of 120 additional RV measurements over the next 1.5 observing seasons for HD 209458 (RA=22:03, DEC=+18:53). Our simulated campaign includes 11 individual RV measurements

cadenced according to typical observing runs on the Keck telescope and 109 RV measurements accumulated over 6 dedicated nights on a smaller instrument such as the Lick Observatory 3-meter telescope. This combination of intensive and sporadic monitoring is intended to improve phase coverage of both planets, while expending a reasonable amount of telescope time.

We then sample the integrated reflex velocity of the star in response to the two planets at each of the 120 epochs in the simulated observing campaign. Gaussian scatter consistent with instrumental error (4.8 m/s) and stellar jitter (4.0 m/s) is added to the sampled stellar reflex velocities. This results in a synthetic data set which includes the 30 real plus 120 simulated RV points. We then perform 1-planet and 2-planet fits to all 150 points. The best 2-planet fit results in a total rms scatter of 6.79 m/s, while the best 1-planet fit results in a scatter of 7.41 m/s, suggesting that a moderately intensive campaign on HD 209458b will result in a slow, but nevertheless feasible discrimination between the 1- and 2-planet hypotheses. Additional Monte-Carlo simulations of this type can be used to further refine the observing strategy. If the eccentricity of the hypothetical planet “c” is larger, as in the fourth fit of Table 3, then the planet will be easier to detect, due to the comparatively larger reflex velocity of the star during the peri-astron passage.

We also note that the time ΔT_c between successive transits for HD 209458b varies by ± 3 s over the course of a single 84 day period of the hypothetical companion. While the average period of HD 209458b can be determined very accurately by spanning a large number of periods (Welsh et al. 2003), it is difficult to obtain 1 s accuracy for the duration of a single orbit. It might be possible, however, to measure precession-induced secular changes in the period of HD 209458b arising from perturbations caused by a second companion (see Miralda-Escudé 2002).

4.2. Ongoing Circularization

The period range between 3 and 10 days is now populated by 16 planets covering a wide range of masses and equilibrium temperatures. Equation (4) indicates that if $Q_P \sim 10^6$, then planets with periods of order 1 week should be in the process of actively circularizing. The circularization timescale, however, depends sensitively on the planetary radius ($\tau_{\text{circ}} \propto R_P^{-5}$), and so among planets with periods of about a week there should be a wide range of non-zero eccentricities, even in the absence of companions capable of forcing eccentricity. There are two additional uncertainties. Tidal dissipation within the host star can also contribute to the evolution of the planet’s eccentricity, although it is smaller than that due to planetary dissipation (Dobbs-Dixon et al 2003). Past tidal inflation instability can also lead to the circularization of planets with $P < 10$ d (Gu et al. 2003). This effect is not important for systems with finite eccentricity. As more planets are discovered in the $3 \text{ d} < P < 10 \text{ d}$ period range, all of the parameters in equation (4) will begin to become overconstrained, eventually allowing $Q_P(T_{\text{eq}}, M_P)$ and $R_P(T_{\text{eq}}, M_P)$ to be observationally determined.

In order to see how the discovery of additional planets with periods of order 1 week will lead

to a better determination for Q_P as a function of planetary mass and temperature, consider Table 4, which lists relevant planetary and stellar information for HD 68988b (Vogt et al. 2002), HD 168746b (Pepe et al. 2002), and HD 217107 (Fischer et al. 1999). In this table, stellar masses, radii and effective temperatures are taken from Allende Prieto & Lambert (1999).

The equilibrium temperature of the planets is calculated as

$$T_{\text{eq}} = \left[\frac{(1 - A)L_\star}{16\pi\sigma a^2(1 + \frac{e^2}{2})^2} \right]^{1/4}, \quad (8)$$

where the quantity $a(1 + e^2/2)$ is the time-averaged distance between the planet and the star for a Keplerian orbit of semi-major axis a and eccentricity e , and A is the Bond albedo for the planet. We adopt $A = 0.4$ when computing the values for T_{eq} listed in Table 4.

The last eight rows of Table 4 show our predictions for the planetary radii and circularization e-folding times. The radii are computed via linear interpolation between the relevant models of Tables 1 and 2, and are coded according to the presence or absence of a core (c/nc) and the presence or absence of kinetic heating (k/nk). Circularization times in each case are computed assuming a fiducial value $Q_P = 10^6$, and $\sin i = 1.0$. Note that τ_{circ} is linearly dependent on Q_P .

With these assumptions, we find that for HD 68988b and HD 217107b, the observationally well-established eccentricities of $e = 0.14$ for both planets are consistent with computed circularization timescales that comfortably exceed the estimated stellar ages. In particular, we note that the non-zero observed eccentricity for HD 68988b is no longer in disagreement with the circularization timescale. A disagreement was noted previously by Vogt et al. (2002), who computed a $\tau_{\text{circ}} = 1.8$ Gyr based on a radius estimate for HD 68988b of $R = 1.4 R_{\text{JUP}}$, motivated by the observed radius for HD 209458b.

We also note that $\dot{E}_d = 2 \times 10^{25}$ and $1 \times 10^{25}(10^6/Q_P)(R_P/R_{\text{JUP}})^5$ erg s^{−1} for HD 68988b and HD 217107b respectively. In contrast, the assumed kinetic energy deposition rate (1% of the irradiation flux) is $\dot{E}_k = 5 \times 10^{26}(R_P/R_{\text{JUP}})^2$ erg s^{−1} for both planets. Even with a modest Q -value (2.5×10^5), \dot{E}_d is an order of magnitude smaller than \dot{E}_k so that tidal dissipation is unlikely to enlarge these planets by a noticeable amount.

For HD 168746, however, the situation is more interesting. Because the planet mass is likely to be small, $M \sin i = 0.23 M_{\text{JUP}}$, there is a large range in the predicted planetary radii depending on the presence of a core and/or kinetic heating, and hence the estimates for τ_{circ} vary widely, from $\tau_{\text{circ}} = 0.26$ Gyr for a core-free model with kinetic heating, to $\tau_{\text{circ}} = 3.5$ Gyr for a model with a core and no kinetic heating. Pepe et al. (2002) estimate that the star HD 168746 is at least several Gyr old, and report an observed eccentricity of $e = 0.081 \pm 0.02$. Using the 154 RVs posted at CDS in conjunction with the Pepe et al. (2002) paper, we confirm that a best-fit $\sqrt{\chi^2} = 1.51$ is obtained for $e = 0.081$, but this value increases to only $\sqrt{\chi^2} = 1.54$ for $e = 0$, indicating that a circular orbit for HD 168746b is still tenable. Improvement of the orbital elements will certainly result as further RV measurements are accumulated.

For this low-mass planet, $\dot{E}_d = 6 \times 10^{24} (10^6/Q_P) (R_P/R_{JUP})^5 \text{ erg s}^{-1}$. We computed two sets (with and without a core of $20 M_\oplus$) of self-consistent models in which uniform tidal dissipation (in accordance with an eccentricity $e = 0.081$) is applied to the planetary interior, with $Q_P = 10^6$, in addition to the surface irradiation (Bodenheimer et al. 2001). Since the radius as a function of time is not known in advance, we iterate the solution until \dot{E}_d at the end of the calculation matches the computed model luminosity. For models with and without cores, $R_P = 1.01 R_{JUP}$ and $1.33 R_{JUP}$ respectively. These tidal models fall between the dissipationless and *ad hoc* kinetic energy dissipation models in the cases both with and without cores. Although the coreless tidal dissipation model gives the same value for R_P as the core-structure model with kinetic energy input, the observational determination of e will remove the degeneracy.

Finally, we remark on the recently reported planet OGLE-TR-56b, $M_p = 0.9 M_{JUP}$, $P = 1.2 \text{ d}$, $T_{eq} = 1,900 \text{ K}$ (Konacki et al. 2003). In comparison with the results in Table 1, the observationally measured $R_P = 1.3 \pm 0.15 R_{JUP}$ is slightly larger than that determined for the irradiated planet with or without a core. But the results in Table 2 indicate that kinetic heating at the rate of 1.7% of the surface irradiative flux induces the planet, with or without a core, to have R_P larger than the observed value. Thus, kinetic heating, if it occurs below the surface of a short-period planet, is less efficient than assumed by Guillot & Showman (2002). We also note that in order to prevent tidal dissipation from expanding R_P beyond its observed value, the eccentricity of OGLE-TR-56b must be less than $1 - 2 \times 10^{-3}$, depending on its Q_P value. If the observed parameters are confirmed, the eccentricity damping time scale of the planet $\tau_{circ} \simeq 1.8(Q_P/10^6) \text{ Myr}$ would be much shorter than the main sequence life span of the host star.

5. Discussion

Our evolutionary models for giant planets indicate that the planetary radius is sensitively dependent on both the presence or absence of a core and on the amount of energy that is deposited within the interior of the planet. This dependence is strongest for hot low-mass (i.e. $M < 1 M_{JUP}$) planets, while being quite weak for planets with large mass (i.e. $M \approx 3 M_{JUP}$) regardless of the equilibrium surface temperature. The discovery of additional extrasolar planets which transit bright parent stars will impart a great deal of information on the structure and evolution of giant planets in general. The number of such planets, however, will be quite limited. The parent star of HD 209458b has $V = 7.65$, yet photometric measurements with HST are photon-limited to a cadence that resolves the critical ingress and egress periods into 80 second time bins (Brown et al. 2001), and a large number of additional RV measurements will be required in order to determine whether the eccentricity of HD 209458b is being forced by a second companion. A similar follow-up effort will be required for additional transiting planets as they are found.

The number of available transiting planets with $3 \text{ d} < P < 200 \text{ d}$ is severely limited by transit probabilities that are generally less than 10%. Information on the interior properties of short-period planets can nonetheless be obtained by examining which of the planetary orbits have been tidally

circularized. Circularization times scale as the fifth power of the planetary radius. As a large aggregate of planets is built up, increasingly stringent limits can be placed on the unknown tidal quality factor Q_P and the planetary radii.

Finally, we note that the discovery of intermediate-period transiting planets is a challenging observational task. The most cost-effective way to find these transiting planets is to harness a network of small independent telescopes to obtain multiple (i.e. 3-5 separate observers) differential-photometric time-series of known planet-bearing stars during the well-defined time windows in which transits are expected to occur. We are currently pursuing this strategy using a network of amateur observers and small-college observatories.²

We thank Richard Freedman for providing us with Rosseland mean opacities for our planetary models. We thank Geoff Marcy for providing us with the latest Keck RV data set for HD 209458 in advance of publication. We thank Debra Fischer, Richard Freedman, Geoff Marcy and Mark Marley for useful conversations. This work was supported in part by a NASA astrophysics theory program which supports a joint Center for Star Formation Studies at NASA-Ames Research Center, UC Berkeley and UC Santa Cruz, by the NASA Origins program through grant NCC2-5501, and by the NSF through grant AST-9987417.

REFERENCES

- Alexander, D. R., & Ferguson, J. W. 1994, *ApJ*, 437, 879
- Allende Prieto, C., & Lambert, D. L. 1999, *A&A*, 352, 555
- Barnes, J. W., & O’Brien, D. P. 2002, *ApJ*, 575, 1087
- Bodenheimer, P., Hubickyj, O., & Lissauer, J. J. 2000, *Icarus*, 143, 2
- Bodenheimer, P., Lin, D. N. C., & Mardling, R. A. 2001, *ApJ*, 548, 466
- Brown, T. M., Charbonneau, D., Gilliland, R. L., Noyes, R. W., & Burrows, A. 2001, *ApJ*, 552, 699
- Bundy, K. A., & Marcy, G. W. 2000, *PASP*, 112, 1421
- Burrows, A., Guillot, T., Hubbard, W. B., Marley, M. S., Saumon, D., Lunine, J. I., & Sudarsky, D. 2000, *ApJ*, 534, L97
- Burrows, A., Hubbard, W. B., Lunine, J. I., & Liebert, J. 2001, *Rev. Mod. Phys.*, 73, 719
- Castellano, T., Jenkins, J., Trilling, D. E., Doyle, L., & Koch, D. 2000, *ApJ*, 532, L51

²<http://www.transitsearch.org>

- Chabrier, G., & Baraffe, I. 2000, *ARA&A*, 38, 337
- Charbonneau, D., Brown, T. M., Latham, D. W., & Mayor, M. 2000, *ApJ*, 529, L45
- Charbonneau, D., Brown, T. M., Noyes, R. W., & Gilliland, R. L. 2002, *ApJ*, 568, 377
- Cody, A. M., & Sasselov, D. D. 2002, *ApJ*, 569, 451
- Dobbs-Dixon, I., Lin, D. N. C., & Mardling, R. A. 2003, *ApJ*, submitted
- Evonuk, M., Lin, D. N. C., & Mardling, R. A. 2003, *ApJ*, submitted
- Fischer, D. A., Marcy, G. W., Butler, R. P., Vogt, S. S., & Apps, K. 1999, *PASP*, 111, 50
- Fischer, D. A., Marcy, G. W., Butler, R. P., Vogt, S. S., Frink, S. F., & Apps, K. 2001, *ApJ*, 551, 1107
- Goldreich, P., & Soter, S. 1966, *Icarus*, 5, 375
- Gu, P. G., Lin, D. N. C., & Bodenheimer, P. 2003, *ApJ*, in press
- Guillot, T., Burrows, A., Hubbard, W. B., Lunine, J. I., & Saumon, D. 1996, *ApJ*, 459, L35
- Guillot, T., & Showman, A. P. 2002, *A&A*, 385, 156
- Henry, G. W., Marcy, G. W., Butler, R. P., & Vogt, S. S. 2000, *ApJ*, 529, L41
- Heney, L. G., Forbes, J. E., & Gould, N. L. 1964, *ApJ*, 139, 306
- Hubbard, W. B., Burrows, A., & Lunine, J. I. 2002, *ARA&A*, 40, 103
- Konacki, M., Torres, G., Jha, S. & Sasselov D. D. 2003 *Nature*, 421, 507
- Laughlin, G., & Chambers, J. E. 2001, *ApJ*, 551, L109
- Lin, D. N. C., Bodenheimer, P., & Richardson, D. C. 1996, *Nature*, 380, 606
- Mardling, R. A., & Lin, D. N. C. 2002, *ApJ*, 573, 829
- Marley, M. S. 1999. In *Encyclopedia of the Solar System*, ed. P. R. Weissman, L. McFadden, & T. V. Johnson (San Diego: Academic Press), p. 339
- Mayor, M., & Queloz, D. 1995, *Nature*, 378, 355
- Mazeh, T., Naef, D., Torres, G., Latham, D. W., Mayor, M. M., Beuzit, J.-L., Brown, T. M., Buchhave, L., Burnet, M., Carney, B. W., Charbonneau, D., Drukier, G. A., Laird, J. B., Pepe, F., Perrier, C., Queloz, D., Santos, N. C., Sivan, J.-P., Udry, S., & Zucker, S. 2000, *ApJ*, 532, L55
- Miralda-Escudé, J. 2002, *ApJ*, 564, 1019

- Murray, C. D., & Dermott, S. F. 1999, *Solar System Dynamics* (Cambridge: Cambridge University Press).
- Pepe, F., Mayor, M., Galland, F., Naef, D., Queloz, D., Santos, N. C., Udry, S., & Burnet, M. 2002, *A&A*, 388, 632
- Pollack, J. B., Hubickyj, O., Bodenheimer, P., Lissauer, J. J., Podolak, M., & Greenzweig, Y. 1996, *Icarus*, 124, 62
- Press, W. H., Teukolsky, S. A., Vetterling, W. T., & Flannery, B. P. 1992, *Numerical Recipes: The Art of Scientific Computing*, 2nd Edition (Cambridge: Cambridge Univ. Press)
- Queloz, D., Eggenberger, A., Mayor, M., Perrier, C., Beuzit, J. L., Naef, D., Sivan, J. P., & Udry, S. 2000, *A&A*, 359, L13
- Robichon, N., & Arenou, F. 2000, *A&A*, 355, 295
- Saar, S. H., Butler, R. P., & Marcy, G. W. 1998, *ApJ*, 498, L153
- Saumon, D., Chabrier, G., & van Horn, H. M. 1995, *ApJS*, 99, 713
- Scargle, J. D. 1982, *ApJ*, 263, 835
- Terquem, C., Papaloizou, J. C. B., Nelson, R. P., & Lin, D. N. C. 1998, *ApJ*, 502, 788
- Tsuji, T. 2002, *ApJ*, 575, 264
- Vogt, S. S., Butler, R. P., Marcy, G. W., Fischer, D. A., Pourbaix, D., Apps, K., & Laughlin, G. 2002, *ApJ*, 568, 352
- Welsh, W. F., et al. 2003, preprint
- Wuchterl, G., Guillot, T., & Lissauer, J. J. 2000, In *Protostars and Planets IV*, ed. V. Mannings, A. P. Boss, & S. S. Russell (Tucson: University of Arizona Press), p. 1081
- Yoder, C. F., & Peale, S. J. 1981, *Icarus*, 47, 1

Fig. 1.— Distribution of 98 planetary periods, $M \sin i$'s, and parent star magnitudes versus date of discovery announcement.

Fig. 2.— Power spectrum of residuals to the best 1-planet fit to HD 209458.

Fig. 3.— Secular exchange of eccentricity in a 2-planet model of the HD 209458b data set. Time is given in years. The solid curves show the eccentricities of planet “b” and the hypothetical planet “c”. The dotted lines show the eccentricity exchange which would occur in the absence of relativistic precession.

TABLE 1: PREDICTED RADII OF IRRADIATED GIANT PLANETS AT T=4.5 GYR

	0.11 M _J		0.23 M _J		0.69 M _J		1.0 M _J		3.0 M _J	
T_{eq}	core	no core	core	no core	core	no core	core	no core	core	no core
2000	0.87	1.75	1.07	1.31	1.10	1.22	1.14	1.20	1.18	1.19
1500	0.74	1.20	0.95	1.14	1.03	1.13	1.08	1.13	1.12	1.13
1000	0.69	1.09	0.90	1.07	1.01	1.10	1.06	1.11	1.11	1.11
500	0.66	1.01	0.88	1.03	1.00	1.09	1.05	1.10	1.10	1.11
113	0.61	0.89	0.82	0.95	0.95	1.03	1.01	1.05	1.07	1.07

TABLE 2: PREDICTED RADII OF IRRADIATED GIANT PLANETS AT T=4.5 GYR
(MODELS WITH KINETIC HEATING)

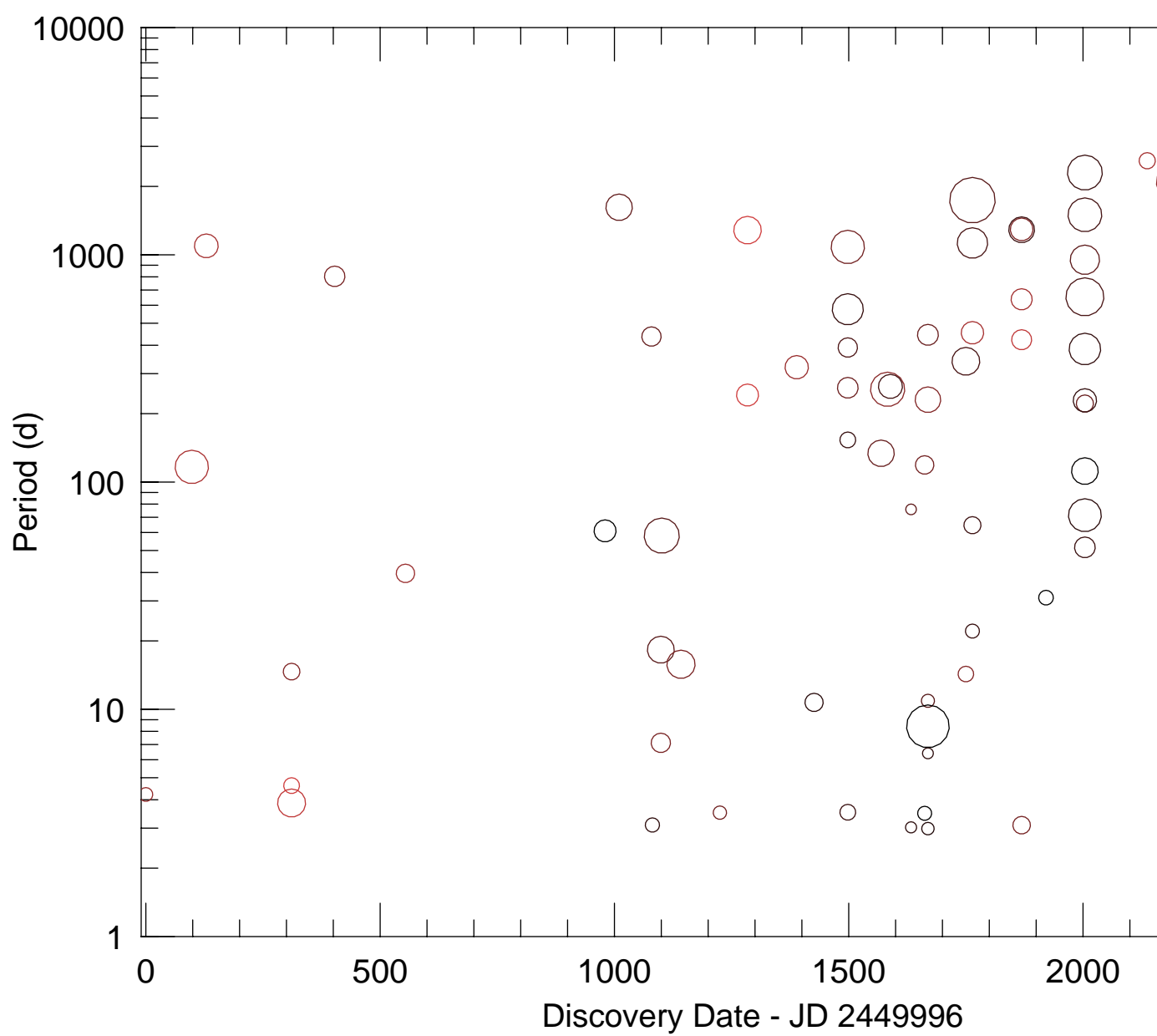
	0.11 M _J		0.23 M _J		0.69 M _J		1.0 M _J		3.0 M _J	
T_{eq}	core	no core	core	no core	core	no core	core	no core	core	no core
2000	>2.0	>2.0	>2.0	>2.0	1.74	1.81	1.47	1.61	1.40	1.35
1500	1.69	>2.0	1.61	1.80	1.35	1.51	1.30	1.38	1.25	1.26
1000	1.14	1.72	1.34	1.53	1.16	1.27	1.13	1.18	1.13	1.14
500	0.80	1.13	1.02	1.14	1.02	1.11	1.06	1.11	1.10	1.11
113	0.61	0.89	0.82	0.95	0.95	1.03	1.01	1.05	1.07	1.07

TABLE 3: TRIAL 2-PLANET FITS TO HD 209458 DATA

Parameter	Fit 1		Fit 2		Fit 3		Fit 4	
	b	c	b	c	b	c	b	c
P (d)	3.5248(f)	84.17	3.5248(f)	84.37	3.5248(f)	84.29	3.5248(f)	84.714
M (deg)	221.85(f)	91.59	221.85(f)	101.22	221.85(f)	104.96	241.57	154.48
e	0.025	0.00(f)	0.022	0.20(f)	0.019	0.40(f)	0.00037	0.697
ϖ	67.58	60.5(f)	67.75	60.5(f)	67.74	60.5(f)	47.6	31.2
$M_{\text{JUP}} \sin(i)$	0.679	0.127(f)	0.679	0.127(f)	0.679	0.127(f)	0.64	0.227

TABLE 4: PLANETS WITH $6\text{d} < P < 8\text{d}$

	HD 68988b	HD 168746	HD 217107
P (d)	6.276	6.403	7.125
K (m/s)	187	28	139.7
$M \sin(i)(M_{\text{JUP}})$	1.80	0.23	1.29
e	0.14	0.081	0.14
M_{\star}/M_{\odot}	1.11	1.04	0.98
$T_{\text{eff}\star}$ (K)	5888	5754	5623
$T_{\text{eq,P}}$ (K)	1004	973	919
R_{\star}/R_{\odot}	1.17	1.07	1.12
Stellar Age (Gyr)	6	> 2 Gyr	5.6
$R_P(\text{c, nk})/R_{\text{JUP}}$	1.08	0.90	1.07
$R_P(\text{nc, nk})/R_{\text{JUP}}$	1.11	1.07	1.11
$R_P(\text{c, k})/R_{\text{JUP}}$	1.13	1.34	1.12
$R_P(\text{nc, k})/R_{\text{JUP}}$	1.17	1.53	1.16
$\tau_{\text{circ}}(\text{c, nk})$ (Gyr)	11.5	3.5	13.9
$\tau_{\text{circ}}(\text{nc, nk})$ (Gyr)	10.1	1.5	11.6
$\tau_{\text{circ}}(\text{c, k})$ (Gyr)	9.2	0.51	10.8
$\tau_{\text{circ}}(\text{nc, k})$ (Gyr)	7.9	0.26	9.1



This figure "fig2.gif" is available in "gif" format from:

<http://arxiv.org/ps/astro-ph/0303541v1>

